153. Chemical Selectivities Disguised by Mass Diffusion. IX. A Simple Model of Mixing-Disguised Reactions in a Continuous, Stirred Tank Reactor[1][2]

10th Communication on the Selectivity of Chemical Processes[1]

by **Hasan Belevi, John R. Bourne** and **Paul Rys**

Technisch-Chemisches Laboratorium, Eidgenössische Technische Hochschule, CH-8092 Zürich

Dedicated to the memory of Prof. *Norbert Ibl*

(13.V.81)

Summary

A mixing-reaction model 'MIRE-CSTR' is developed to describe the selectivity behaviour of mixing-disguised reactions in continuous stirred tank reactors (CSTR). For competitive, consecutive reactions the general behaviour is demonstrated and a comparison with the behaviour in discontinuous operation is made. Furthermore, the start-up process of the CSTR is discussed with the help of a model similar to the model 'MIRE-CSTR'.

1. Introduction. – In order to carry out a chemical reaction, the reacting species must first be mixed together. A coarse grained distribution of the liquid zones is achieved by convection (macromixing), and the equalisation of the concentrations on the molecular scale is achieved by molecular diffusion (micromixing).

During kinetic investigations of a chemical transformation the mixing process must be considered, if the characteristic times of these processes are of the same order or if the mixing time is greater than the characteristic time of the actual chemical reaction (reorganisation of the chemical bonds).

Several models have been developed to describe the coupling between the mixing-process and the chemical reaction[3]. One of these is the mixing-reaction model MIRE [3–6], developed from a more general diffusion-immobilization theory [7] [8]. The MIRE-model has been previously applied to describe discontinuous reactions. Here, it will be developed to describe the behaviour of mixing-disguised reactions in a continuous stirred tank reactor (CSTR) in steady-state. In this type of operation the reactants A and B flow continuously into the reactor, and the products R and S as well as those reactants which have not reacted flow continuously out of the reactor.

[1] Part VIII and 9th Communication *cf.* [1].
[2] Results taken from the Ph. D. thesis of *H. Belevi* [2].
[3] A summary of these models is given in [9].

0018-019X/81/5/1630-15$01.00/0

2. Diffusion-Reaction Model MIRE-CSTR. - Here, the mixing-reaction model MIRE-CSTR will be developed for the competitive, consecutive reactions *(Scheme).*

Scheme

$$A + B \xrightarrow{k_1} R$$

$$R + B \xrightarrow{k_2} S$$

During the addition of a solution of the species A and a solution of the species B to a stirred solution in the reactor, eddies rich in A and B are created in the stirred solution. By the theory of turbulence [10] one can estimate the minimum mean size of the eddies from the size of the *Kolmogoroff* velocity microscale λ_K.

If the assumption can be made that the macromixing is much faster than micromixing [11], the concentration gradient between the surface of the eddies and the surrounding solution can be neglected. Consequently, the concentrations at the interface of the eddies correspond to those in the surrounding solution at any time.

In order to make the simulation of the mixing-reaction process by numerical computation simpler[4]), the reactant B is considered to be immobile and the reactant A as well as the products R and S are considered to be mobile. While the species B is fixed in the B-eddy[5]), the species A, R and S can diffuse within the eddies as well as through the interface.

In general, the molar feed rates of the solutions A and B are so chosen, that the species B is not in excess. Assuming that, up to 100% conversion of B, the B-eddies remain spherical with a constant radius[6]), the species B exists neither in the surrounding solution nor in the A-eddy.

Since the species B is assumed to be immobilized in the B-eddy, the model restricts itself to the diffusion-reaction process in the B-eddy.

The unsteady character of the diffusion-reaction process and the steady character of the CSTR require a discretisation of the continuous operation. Therefore, the continuous operation is discretised into time-intervals τ_E, whereby τ_E represents the time, which passes from the formation to the disappearance of the B-eddy. The time t in this conception is then a measure of the age of an eddy since its formation.

In a time-interval τ_E diffusion and reaction proceed discontinuously (batchwise). This conception requires some additional assumptions *(Fig. 1).*

- Before the addition of the feed solutions *(state I)*, only the species A, R and S exist in the reactor, because of the complete conversion of species B in the previous discretization interval.

---

4) This simplification reduces substantially the time for computer calculations without falsifying the general qualitative conclusions about mixing effects in fast reactions.

5) The B-eddy and the A-eddy are eddies, which at the start of the diffusion-reaction process only consist of species B and species A, respectively.

6) Calculations have shown that linear, cylindrical or time-dependent geometries give other results. Because of the higher surface-to-volume ratio, every other geometry of the eddy having the same volume shows a lower disguising effect of diffusion on the selectivity. However, the general behaviour is the same. A comprehensive discussion is in preparation.

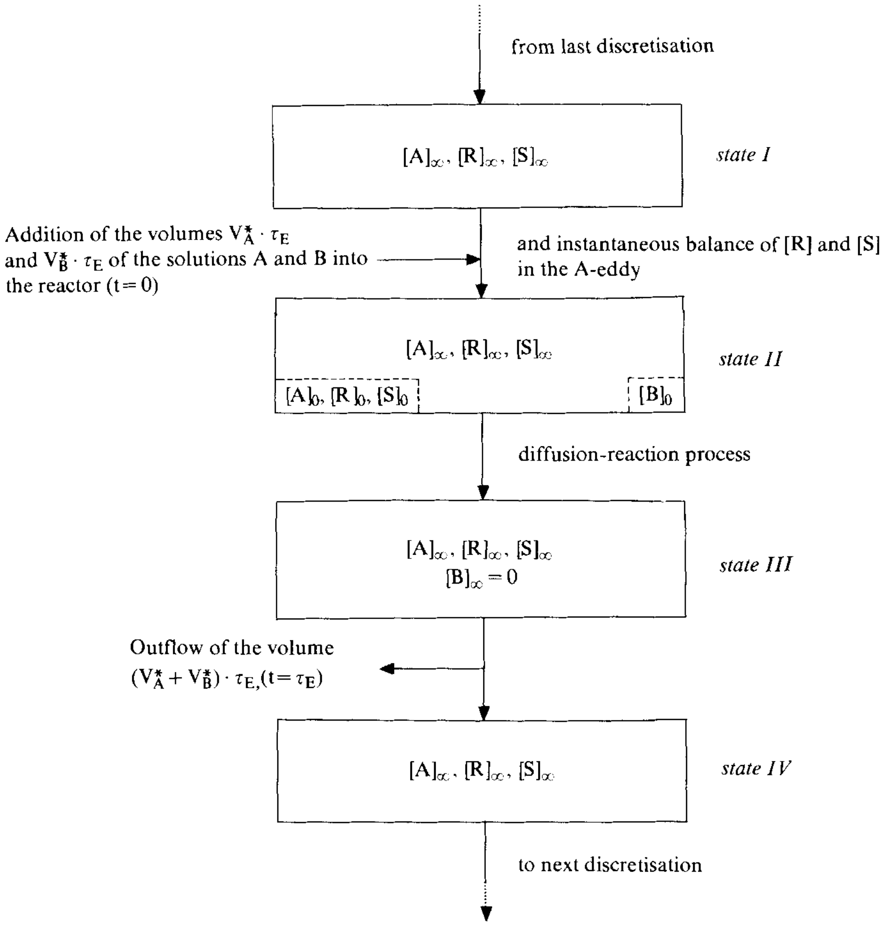

Fig. 1. *Discretisation of the continous operation* (newly entered solutions of A and B)

- After the addition of the solutions A and B (t=0), the concentrations of R and S in the A-eddy are reached instantaneously *(state II)*.
- The diffusion-reaction process occurs only in the B-eddy, into which the species A diffuses and reacts to R and S. Furthermore, the species A also diffuses out of the A-eddy keeping the concentration of A in the surrounding solution constant ($[A]=[A]_\infty$). After 100% conversion of B *(state III)*, the concentrations of A, R and S at any point in the reactor are homogeneous and $[B]_\infty=0$. The concentrations of R and S are greater than at the start of the diffusion-reaction process. This difference corresponds to the amount, which flows out of the reactor during the time τ_E in continuous operation[7]).
- Finally, a volume $V^* \cdot \tau_E$, which corresponds to the feed volume flows instantaneously out of the reactor leading to *state IV*, which corresponds to *state I* of the next discretization interval.

[7]) The unsteady concentrations of R and S in this representation result from the discretisation.

3. Mathematical Description of the Mixing-Reaction-Process. - Equation 1 describes the change of the molar concentration of the component i with respect to time at any point r ($\leq \bar{R}$).

$$\frac{\partial [i]}{\partial t} = D_{i}\left(\frac{\partial^{2} [i]}{\partial r^{2}} + \frac{2}{r}\frac{\partial [i]}{\partial r}\right) + \boldsymbol{r}_{i} \tag{1}$$

One obtains this equation with the help of a material balance for all the species under the following restrictions [3]:
- Isothermal system
- Incompressible liquid
- Dilute solutions
- Spherical eddy of constant size

For the species *B*, which is assumed to be immobile, the diffusivity D_B is 0.

Replacing the molar rate of production by chemical reaction $\boldsymbol{r}_i$ by the corresponding kinetic equations, one obtains the following diffusion-reaction equations:

$$\frac{\partial [A]}{\partial t} = D\left(\frac{\partial^{2} [A]}{\partial r^{2}} + \frac{2}{r}\frac{\partial [A]}{\partial r}\right) - k_{1}[A][B] \tag{2}$$

$$\frac{\partial [R]}{\partial t} = D\left(\frac{\partial^{2} [R]}{\partial r^{2}} + \frac{2}{r}\frac{\partial [R]}{\partial r}\right) + k_{1}[A][B] - k_{2}[R][B] \tag{3}$$

$$\frac{\partial [S]}{\partial t} = D\left(\frac{\partial^{2} [S]}{\partial r^{2}} + \frac{2}{r}\frac{\partial [S]}{\partial r}\right) + k_{2}[R][B] \tag{4}$$

$$\frac{\partial [B]}{\partial t} = -k_{1}[A][B] - k_{2}[R][B] \tag{5}$$

For simplicity, the diffusing species are now considered to have a common diffusivity *D*.

One boundary condition for each partial differential equation results from the fact, that no concentration gradient arises at the center of the eddy owing to the symmetry of the sphere.

$$r = 0: \frac{\partial [A]}{\partial r} = \frac{\partial [R]}{\partial r} = \frac{\partial [S]}{\partial r} = 0 \tag{6}$$

The concentration of the species A at the surface of the eddy is constant during the time τ_E. Thus a further boundary condition results for the species A:

$$r = \bar{R}: [A] = [A]_{\infty} \tag{7}$$

The boundary conditions for R and S ensue from the requirement, that the change of the amount of dissolved species R and S in the surrounding solution

(A-eddy included) has to correspond to the flux of R and S, which diffuses through the surface of the B-eddy:

$$r=\bar{R}: \frac{\partial [R]}{\partial t} = -3 \frac{V_B}{V_A} \frac{D}{\bar{R}} \frac{\partial [R]}{\partial r} \tag{8}$$

$$\frac{\partial [S]}{\partial t} = -3 \frac{V_B}{V_A} \frac{D}{\bar{R}} \frac{\partial [S]}{\partial r} \tag{9}$$

The initial conditions (t=0) result from the state of the mixture immediately after the complete segregation at the beginning of the time-interval τ_E *(Fig. 1)*.

$$r<\bar{R}: \quad [A]=0; \quad [R]=0; \quad [S]=0; \quad [B]=[B]_0 \tag{10}$$

$$r=\bar{R}: \quad [A]=[A]_\infty; \quad [R]=[R]_0; \quad [S]=[S]_0; \quad [B]=[B]_0 \tag{11}$$

4. Procedure for Numerical Solution. – For the complete description of the diffusion-reaction process 2–11 the parameters $[A]_\infty$, $[R]_0$, $[S]_0$ and $\boldsymbol{\alpha}$ must be calculated. $[R]_0$ and $[S]_0$ are given by the equations 12 and 13, which result from the mass balances as a function of $[A]_\infty$ (see *Appendix*).

$$[R]_0=\left(1-\frac{\boldsymbol{\alpha}_z}{\boldsymbol{\alpha}}\right)\left(\frac{2\,V_A^*[A]_0 - V_B^*[B]_0}{V_A^*+V_B^*} - 2[A]_\infty\right) \tag{12}$$

$$[S]_0=\left(1-\frac{\boldsymbol{\alpha}_z}{\boldsymbol{\alpha}}\right)\left(\frac{V_B^*[B]_0 - V_A^*[A]_0}{V_A^*+V_B^*} + [A]_\infty\right) \tag{13}$$

The ratio $\boldsymbol{\alpha}$ of the surrounding solution volume (A-eddy included) to the B-eddy volume is given by the following relation:

$$\boldsymbol{\alpha} = \frac{V_K - V_B}{V_B} = \frac{\tau\,(V_A^*+V_B^*) - V_B}{V_B} \tag{14}$$

Furthermore, $V_B = \tau_E \cdot V_B^*$ (see *Appendix*). Introducing this into equ. 14 leads to:

$$\boldsymbol{\alpha} = \frac{\tau}{\tau_E}(1+\boldsymbol{\alpha}_z) - 1 = \gamma\,(1+\boldsymbol{\alpha}_z) - 1 \tag{15}$$

$\boldsymbol{\alpha}$ can be calculated by estimating γ. As it is assumed that $\tau \rangle\rangle \tau_E$, γ is very large. The calculations have shown, that the product distribution remains constant for values of γ which are greater than 10.

The product distribution X_S in the product stream is given by the following relation:

$$X_S = \frac{2[S]_\infty}{[R]_\infty + 2[S]_\infty} \tag{16}$$

X_S follows from the solution of the diffusion-reaction-equations 2–5, as well as from the equation 17 which results from the mass balances (see *Appendix*).

$$X_S = 2 - 2\boldsymbol{E} \cdot \boldsymbol{\alpha}_z + 2\boldsymbol{E}(1 + \boldsymbol{\alpha}_z)\frac{[A]_\infty}{[A]_0} \tag{17}$$

The requirement, that the product distribution X_S calculated by the both methods has to be equal, enables an iterativ solution.

The diffusion-reaction equations can not be solved analytically. Therefore, a computer program was written in FORTRAN, whereby, for the solution of the partial differential equations, the subroutines of the simulation package FORSIM-V were used [2]. The calculations were carried out on a CDC computer.

5. Calculation of the Concentration of B in the Product Stream. - Although the model MIRE-CSTR assumes that $[B]_\infty = 0$, a part of the eddies leave the CSTR during the time-interval τ_E. Since the diffusion-reaction process has not expired then, there is a certain concentration of species B in the product stream.

The part $\boldsymbol{\delta}$ of the eddies which have a residence time smaller than τ_E can be calculated by the relation 18 [12].

$$\boldsymbol{\delta} = 1 - \exp\left(-\frac{\tau_E}{\tau}\right) = 1 - \exp\left(-\frac{1}{\gamma}\right) \tag{18}$$

The concentration of B in the product stream is given by the ratio of the quantity of species B to the volume of solution, which leaves the reactor during τ_E.

$$[B]_\infty = \frac{1 - e^{-1/\gamma}}{1 + \boldsymbol{\alpha}_z}\,\frac{3}{\bar{R}^3}\,\frac{1}{\tau_E}\int_0^{\tau_E}\int_0^{\bar{R}} [B]\, r^2\, dr\, dt \tag{19}$$

Thus, the conversion of B can be calculated by the equation 20.

$$X_B = 1 - (1 - e^{-1/\gamma})\,\frac{3}{\bar{R}^3}\,\frac{1}{\tau_E}\int_0^{\tau_E}\int_0^{\bar{R}} \frac{[B]}{[B]_0}\, r^2\, dr\, dt \tag{20}$$

6. Results. - For steady operation of a CSTR with given initial and boundary conditions, the product distribution X_S is a function of $\boldsymbol{E}$, $\boldsymbol{\alpha}_z$, $\boldsymbol{\varphi}^2_{B,1}$, $\boldsymbol{\varphi}^2_{B,2}$ and γ. $\boldsymbol{\varphi}^2_{B,1}$ and $\boldsymbol{\varphi}^2_{B,2}$ are mixing moduli, given by the relations 21 and 22.

$$\boldsymbol{\varphi}^2_{B,1} = \frac{k_1 \bar{R}^2 [B]_0}{D} \tag{21}$$

$$\boldsymbol{\varphi}^2_{B,2} = \frac{k_2 \bar{R}^2 [B]_0}{D} \tag{22}$$

These expressions correspond to the *Damköhler*-Number [13], to the square of '*Thiele*-Modulus' [14] and to the '*Hatta*-Number' [15] respectively, and are proportional to the ratio of the relaxation times of diffusion and chemical reaction.

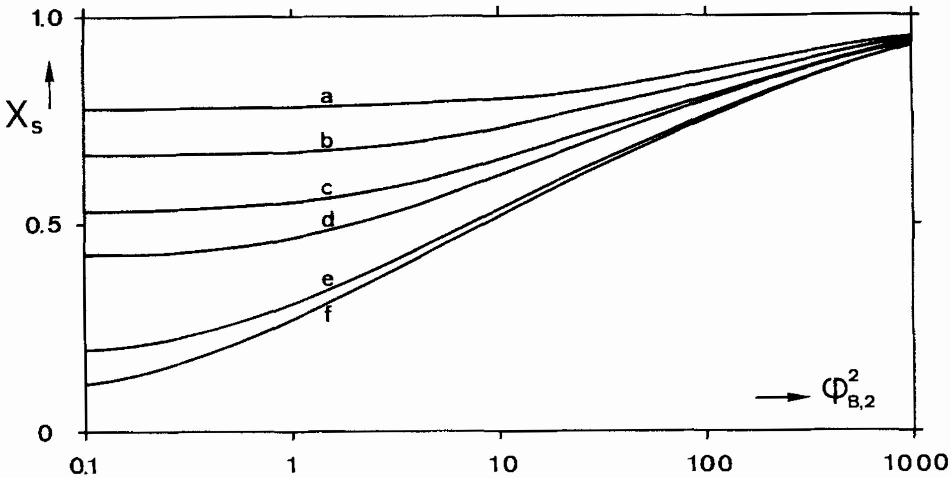

Fig. 2. *Model calculations with MIRE-CSTR: X_S as a function of $\varphi^2_{B,2}$ for different (a–f) selectivities $\varphi^2_{B,1}/\varphi^2_{B,2}$*

$E = 1$; $\alpha_z = 1$; $\gamma = 100$; $\varphi^2_{B,1}/\varphi^2_{B,2} = 1$ (a); 2 (b); 5 (c); 10 (d); 100 (e); 1000 (f).

The selectivity behaviour of mixing-disguised competitive, consecutive reactions in a CSTR are shown in *Figures 2–4* and in *Tables* 1–5.

Figure 2 shows the influence of the mixing moduli $\varphi^2_{B,1}$ and $\varphi^2_{B,2}$. With an increase of $\varphi^2_{B,2}$, the effect of mixing increases and the product distribution X_S becomes greater. When $\varphi^2_{B,2}$ approaches infinity, only the product S arises and X_S becomes 1. On the other hand, X_S tends to the reaction controlled value for very small values of $\varphi^2_{B,2}$. With increasing values of the ratio $\varphi^2_{B,1}/\varphi^2_{B,2}$ the product

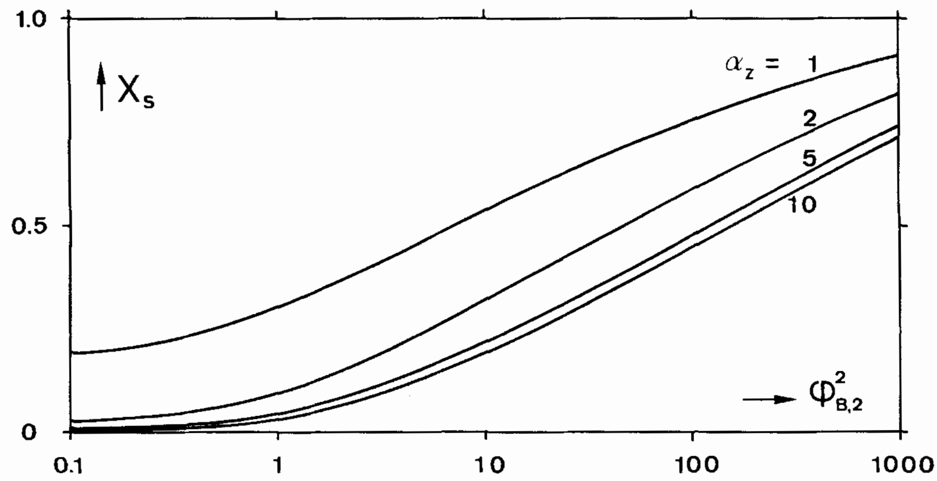

Fig. 3. *Model calculations with MIRE-CSTR: X_S as a function of $\varphi^2_{B,2}$ for different values of α_z*

$E = 1$; $\varphi^2_{B,1}/\varphi^2_{B,2} = 100$; $\gamma = 100$.

Table 1. *Model calculations with MIRE-CSTR: X_S as a function of $\varphi^2_{B,2}$ for different selectivities* $\varphi^2_{B,1}/\varphi^2_{B,2}$ (RC: reaction-controlled)

E	α_z	γ	$\frac{\varphi^2_{B,1}}{\varphi^2_{B,2}}$	$\varphi^2_{B,2}$	X_S
1	1	100	1	RC	0.764
				1	0.771
				10	0.800
				100	0.869
				1000	0.950
1	1	100	2	RC	0.667
				1	0.675
				10	0.737
				100	0.837
				1000	0.942
1	1	100	5	RC	0.528
				1	0.555
				10	0.657
				100	0.805
				1000	0.930
1	1	100	10	RC	0.425
				1	0.470
				10	0.610
				100	0.789
				1000	0.922
1	1	100	100	RC	0.174
				0.1	0.197
				1	0.306
				10	0.536
				100	0.756
				1000	0.918
1	1	100	1000	RC	0.060
				0.1	0.118
				1	0.271
				10	0.617
				100	0.750
				1000	0.915

distribution X_S decreases. The greater the value of $\varphi^2_{B,2}$ the less the ratio $\varphi^2_{B,1}/\varphi^2_{B,2}$ will affect X_S.

Nabholz et al. established the same effects for discontinuous operation [4]. A comparison of these results with the values in *Figure 2* shows, that the values of X_S in a CSTR are generally larger than those in a batch reactor. The more one moves from the reaction controlled regime to the diffusion controlled regime, the smaller will be this difference. More detailed comparison between discontinuous and continuous operation is given in [9].

For a constant ratio of feed concentrations $\boldsymbol{E}$, the product distribution X_S decreases with increasing ratio of the volumetric feed rates $\boldsymbol{\alpha}_z$ *(Fig. 3)*. Furthermore, the product distribution increases with decreasing values of $\boldsymbol{E}$ for a given value of $\boldsymbol{\alpha}_z$ *(Fig. 4)*. For the constant stoichiometric ratio of the reactant solutions $\boldsymbol{E} \cdot \boldsymbol{\alpha}_z$ the

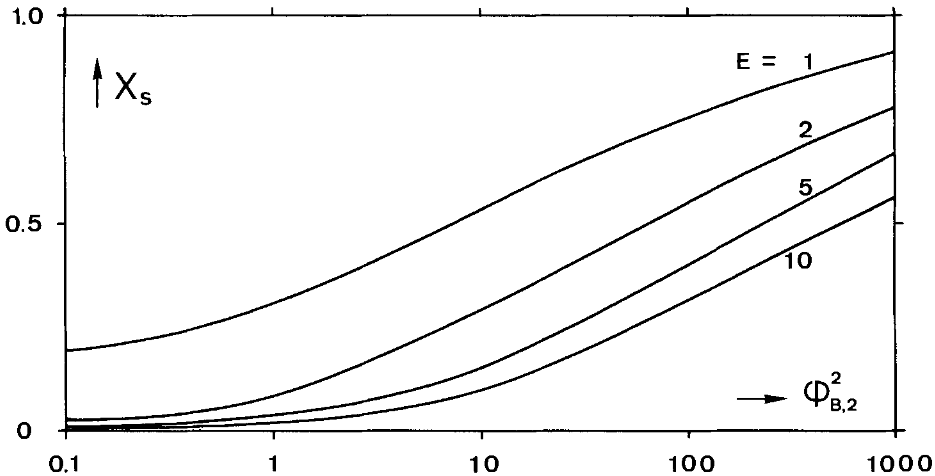

Fig. 4. *Model calculations with MIRE-CSTR: X_S as a function of $\varphi^2_{B,2}$ for different values of E*
$\alpha_z = 1$; $\varphi^2_{B,1}/\varphi^2_{B,2} = 100$; $\gamma = 100$.

mixing effect increases with increasing values of α_z, and X_S becomes greater *(Table 4)*. γ-values, which are greater than a characteristic value, have no appreciable influence on the product distribution. For $E = 1$, $\alpha_z = 1$ and $\varphi^2_{B,1}/\varphi^2_{B,2} = 100$, this value is at $\gamma = 10$ *(Table 5)*.

Table 6 shows the dependence of the concentration of B in the product stream and of the conversion of B in the reactor on γ, for a parameter set E, α_z, $\varphi^2_{B,1}$ and

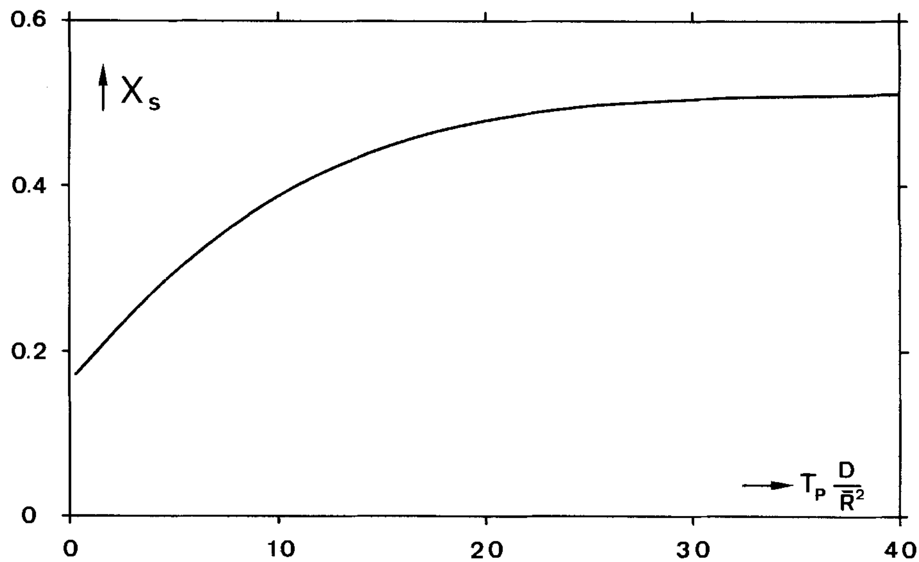

Fig. 5. *Model calculations with MIRE-IND for the start-up process: X_S as a function of $\tau_P \cdot (D/\bar{R}^2)$*
$E = 1$; $\alpha_z = 1$; $\varphi^2_{B,1} = 1000$; $\varphi^2_{B,2} = 10$; $\gamma = 10$.

Table 2. *Model calculations with MIRE-CSTR: X_S as a function of $\varphi^2_{B,2}$ for different values of α_z* (RC: reaction-controlled)

E	α_z	γ	$\frac{\varphi^2_{B,1}}{\varphi^2_{B,2}}$	$\varphi^2_{B,2}$	X_S
1	1	100	100	RC	0.174
				0.1	0.197
				1	0.306
				10	0.536
				100	0.756
				1000	0.918
1	2	100	100	RC	0.019
				0.1	0.032
				1	0.095
				10	0.320
				100	0.590
				1000	0.820
1	5	100	100	RC	0.005
				0.1	0.013
				1	0.048
				10	0.220
				100	0.480
				1000	0.750
1	10	100	100	RC	0.002
				0.1	0.007
				1	0.038
				10	0.190
				100	0.452
				1000	0.715

Table 3. *Model calculations with MIRE-CSTR: X_S as a function of $\varphi^2_{B,2}$ for different values of E* (RC: reaction-controlled)

E	α_z	γ	$\frac{\varphi^2_{B,1}}{\varphi^2_{B,2}}$	$\varphi^2_{B,2}$	X_S
1	1	100	100	RC	0.174
				0.1	0.197
				1	0.306
				10	0.536
				100	0.756
				1000	0.918
2	1	100	100	RC	0.019
				0.1	0.030
				1	0.082
				10	0.290
				100	0.550
				1000	0.790
5	1	100	100	RC	0.005
				0.1	0.010
				1	0.032
				10	0.153
				100	0.395
				1000	0.661

Table 3 (continued)

E	α_z	γ	$\frac{\varphi^2_{B,1}}{\varphi^2_{B,2}}$	$\varphi^2_{B,2}$	X_S
10	1	100	100	RC	0.002
				0.1	0.008
				1	0.019
				10	0.098
				100	0.315
				1000	0.563

$\varphi^2_{B,2}$. From $\gamma = 10$ on, the concentration of B in the product stream is very small. In practice, γ in a CSTR is mostly much higher than 10 [9]. Consequently, the assumption of complete conversion of B in the reactor is justified.

A similar model to MIRE-CSTR was developed to describe the start-up of a CSTR [2]. *Figure 5* represents a start-up process, in which at the beginning the solution in the CSTR consists only of the species A. The appropriate values are listed in *Table 7.*

Table 4. *Model calculations with MIRE-CSTR: X_S as a function of $\varphi^2_{B,2}$ for different values of α_z at constant values for $E \cdot \alpha_z$*
(RC: reaction-controlled)

E	α_z	γ	$\frac{\varphi^2_{B,1}}{\varphi^2_{B,2}}$	$\varphi^2_{B,2}$	X_S
2	0.5	100	100	RC	0.174
				0.1	0.197
				1	0.303
				10	0.527
				100	0.740
				1000	0.897
1	1	100	100	RC	0.174
				0.1	0.197
				1	0.306
				10	0.536
				100	0.756
				1000	0.918
0.5	2	100	100	RC	0.174
				0.1	0.198
				1	0.310
				10	0.545
				100	0.774
				1000	0.927
0.2	5	100	100	RC	0.174
				0.1	0.198
				1	0.312
				10	0.556
				100	0.797
				1000	0.955

Table 5. *Model calculations with MIRE-CSTR: X_S as a function of $\varphi^2_{B,2}$ for different values of γ*

E	α_z	γ	$\frac{\varphi^2_{B,1}}{\varphi^2_{B,2}}$	$\varphi^2_{B,2}$	X_S
1	1	1	100	0.1	0.144
				1	0.244
				10	0.490
				100	0.723
				1000	0.878
1	1	2	100	0.1	0.173
				1	0.278
				10	0.517
				100	0.742
				1000	0.896
1	1	5	100	0.1	0.188
				1	0.296
				10	0.529
				100	0.749
				1000	0.905
1	1	10	100	0.1	0.193
				1	0.301
				10	0.533
				100	0.754
				1000	0.916
1	1	100	100	0.1	0.197
				1	0.306
				10	0.536
				100	0.756
				1000	0.918
1	1	1000	100	0.1	0.197
				1	0.306
				10	0.536
				100	0.756
				1000	0.918

The steady-state was reached when $\tau_P = 40\ \bar{R}^2/D$. τ_P is the process time, which elapses since the entry of the first eddy into the reactor.

By the assumption, that τ_E is of the same order as $\bar{R}^2/D$, $\tau_P = 40 \cdot \tau_E$. Since in the calculations $\tau/\tau_E = 10$, the steady state will first be reached after some 4 mean residence times.

7. Conclusions. - The influence of micromixing on the product distribution of mixing-disguised reactions in a CSTR has been simulated with the help of a mixing-reaction model MIRE-CSTR. The general behaviour of a mixing-disguised competitive consecutive reaction in a CSTR is determined for given initial and boundary conditions by the five parameters $\boldsymbol{E}$, $\boldsymbol{\alpha}_z$, $\varphi^2_{B,1}$, $\varphi^2_{B,2}$ and γ. These parameters determine to what extent the intrinsic product distribution will be disguised by diffusion. The same general trends regarding the selectivity behaviour are evident as for mixing-disguised discontinuous reactions [3] [4].

Further investigations will show the conformity of the experimental results with the results, which are calculated by MIRE-CSTR.

Table 6. *Model calculations with MIRE-CSTR:* $\boldsymbol{B}_{B,\infty}$ *and* X_B *as a function of* γ
$\boldsymbol{E}=1$; $\boldsymbol{\alpha}_z=1$; $\varphi^2_{B,1}=1000$; $\varphi^2_{B,2}=10$

γ	$\boldsymbol{B}_{B,\infty}$	X_B	γ	$\boldsymbol{B}_{B,\infty}$	X_B
1	0.0560	0.888	20	0.0047	0.990
2	0.0406	0.919	50	0.0019	0.996
5	0.0180	0.964	100	0.0010	0.998
10	0.0092	0.982	1000	0.0001	0.9998

Table 7. *Model calculations with MIRE-IND for the start-up process:* X_S *as a function of* $\tau_P(D/\bar{R}^2)$
$\boldsymbol{E}=1$; $\boldsymbol{\alpha}_z=1$; $\varphi^2_{B,1}=1000$; $\varphi^2_{B,2}=10$; $\gamma=10$

$\tau_P(D/\bar{R}^2)$	X_S	$\tau_P(D/\bar{R}^2)$	X_S	$\tau_P(D/\bar{R}^2)$	X_S
0.25	0.171	8.14	0.359	20.99	0.482
0.51	0.178	8.72	0.369	21.72	0.485
0.79	0.185	9.32	0.379	22.46	0.488
1.08	0.193	9.94	0.389	23.20	0.490
1.38	0.201	10.57	0.399	23.94	0.492
1.71	0.210	11.21	0.406	24.68	0.494
2.05	0.219	11.86	0.415	25.42	0.496
2.41	0.228	12.52	0.422	26.17	0.497
2.78	0.238	13.19	0.430	26.92	0.499
3.18	0.249	13.87	0.436	27.66	0.500
3.59	0.259	14.56	0.443	28.41	0.501
4.02	0.270	15.25	0.449	29.16	0.502
4.48	0.281	15.95	0.454	29.92	0.503
4.95	0.292	16.66	0.459	30.67	0.504
5.43	0.304	17.37	0.464	31.42	0.505
5.94	0.315	18.08	0.468	32.18	0.506
6.46	0.326	18.80	0.472	32.93	0.506
7.00	0.338	19.53	0.476	33.68	0.507
7.56	0.348	20.26	0.479	34.44	0.507

Appendix

The following mass balances are valid over the CSTR.

$$V^*_A[A]_0=(V^*_A+V^*_B)([A]_\infty+[R]_\infty+[S]_\infty) \tag{23}$$

$$V^*_B[B]_0=(V^*_A+V^*_B)([B]_\infty+[R]_\infty+2[S]_\infty) \tag{24}$$

Combining these equations and assuming $[B]_\infty=0$ one obtains:

$$[R]_\infty=\frac{2V^*_A[A]_0-V^*_B[B]_0}{V^*_A+V^*_B}-2[A]_\infty \tag{25}$$

$$[S]_\infty=\frac{V^*_B[B]_0-V^*_A[A]_0}{V^*_A+V^*_B}+[A]_\infty \tag{26}$$

When the steady state in the CSTR has been reached, the amounts of R and S, which arise during the diffusion-reaction process, have to equal the amounts of R and S, which flowed during τ_E out of the CSTR. Hence further mass balances follow:

$$(V_A^* + V_B^*)\tau_E[R]_\infty = (V_A + V_B)[R]_\infty - V_A[R]_0 \tag{27}$$

$$(V_A^* + V_B^*)\tau_E[S]_\infty = (V_A + V_B)[S]_\infty - V_A[S]_0 \tag{28}$$

The volume V_B of the feed stream B, which flows during τ_E into the CSTR, is

$$V_B = V_B^* \cdot \tau_E \tag{29}$$

The equations 25–29 enable one to represent the concentrations $[R]_0$ and $[S]_0$ as functions of $[A]_\infty$.

$$[R]_0 = \left(1 - \frac{\alpha_z}{\alpha}\right)\left(\frac{2V_A^*[A]_0 - V_B^*[B]_0}{V_A^* + V_B^*} - 2[A]_\infty\right) \tag{12}$$

$$[S]_0 = \left(1 - \frac{\alpha_z}{\alpha}\right)\left(\frac{V_B^*[B]_0 - V_A^*[A]_0}{V_A^* + V_B^*} + [A]_\infty\right) \tag{13}$$

List of Symbols

A	Species A, reagent in *Scheme*
B	Species B, reagent in *Scheme*
$B_{B,\infty}$	Concentration of B after $t \to \infty$ normalized with respect to $[B]_0$.
D_i	Diffusivity of i $[m^2 \cdot s^{-1}]$
E	Ratio of the initial concentration of A and B, $[A]_0/[B]_0$
i	Species i
k_1, k_2	Intrinsic rate constants $[dm^3 \cdot mol^{-1} \cdot s^{-1}]$
R	Species R, primary reaction product in *Scheme*
$\bar{R}$	Radius of spherical eddy [m]
r	Radial coordinate within spherical eddy [m]
r_i	Specific reaction rate of substance i $[mol \cdot dm^{-3} \cdot s^{-1}]$
S	Species S, secondary reaction product in *Scheme*
t	Age of B-eddy [s]
V_A	Volume of surrounding solution and A-eddy $[m^3]$
V_B	Volume of B-eddy $[m^3]$
V_K	Total volume of solution in reactor $[m^3]$
V_A^*	Volumetric flow rate of solution A $[m^3 \cdot s^{-1}]$
V_B^*	Volumetric flow rate of solution B $[m^3 \cdot s^{-1}]$
X_B	Conversion of B
X_S	Measure of product distribution, defined in equ. (16)
α	Ratio of volumes in CSTR, V_A/V_B
α_z	Ratio of volumetric feed rates, V_A^*/V_B^*
γ	Ratio of mean residence time to time for diffusion and reaction in the B-eddy, τ/τ_E
δ	Fraction of eddies, which have a residence time smaller than τ_E
λ_K	*Kolmogoroff* velocity microscale [m]
τ	Mean residence time in a CSTR [s]
τ_E	Time for diffusion and reaction in the B-eddy [s]
τ_P	Process time, measured from start-up [s]
$\varphi_{B,1}^2, \varphi_{B,2}^2$	Normalized rate constants, defined in equ. 21 and 22 (= Mixing-Moduli)

Special Notation

[i]	Concentration of species i $[mol \cdot dm^{-3}]$
$[i]_0$	Initial concentration of species i $[mol \cdot dm^{-3}]$
$[i]_\infty$	Concentration of species i in product stream $[mol \cdot dm^{-3}]$

REFERENCES

[1] *H. Belevi, J.R. Bourne & P. Rys,* Helv. Chim. Acta *64,* 1618 (1981).
[2] *H. Belevi,* Ph. D. thesis ETH, Zurich 1980.
[3] *R.J. Ott & P. Rys,* Helv. Chim. Acta *58,* 2074 (1975).
[4] *F. Nabholz, R.J. Ott & P. Rys,* Helv. Chim. Acta *60,* 2926 (1977).
[5] *F. Nabholz & P. Rys,* Helv. Chim. Acta *60,* 2937 (1977).
[6] *J.R. Bourne, E. Crivelli & P. Rys,* Helv. Chim. Acta *60,* 2944 (1977).
[7] *R.J. Ott & P. Rys,* J. Chem. Soc., Faraday I *69,* 1694, 1775 (1973).
[8] *R.J. Ott & P. Rys,* ibid. *70,* 985, 995 (1974).
[9] *J.R. Bourne, F. Kozicki & P. Rys,* Chem. Eng. Sci. **36**, in press (1981); *H. Belevi, J.R. Bourne & P. Rys,* ibid. **36**, in press (1981); *J.R. Bourne, U. Moergeli & P. Rys,* ibid. **36**, in press (1981).
[10] *A.N. Kolmogoroff,* C. R. Acad. Sci. USSR *30,* 301 (1941).
[11] *V.G. Levich,* 'Physico Chemical Hydrodynamics', Prentice Hall, New York 1962, p. 20.
[12] *P.V. Danckwerts,* Chem. Eng. Sci. *2,* 1 (1953).
[13] *G. Damköhler,* «Einfluss von Diffusion, Strömung und Wärmetransport auf die Ausbeute bei chemisch-technischen Reaktoren», Der Chemieingenieur III-1, Akad. Verlagsges., Leipzig 1937.
[14] *E.W. Thiele,* Chem. Technol. *31,* 916 (1939).
[15] *S. Hatta,* Tohoku Imperial U. Techn. Repts. *10,* 119 (1932).